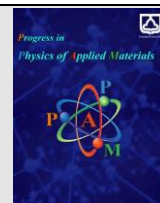




Semnan University



Surface characterization of Al thin film dependent on the substrate using fractal geometry

Mahsa Fakharpour^{a*}, Maryam Gholizadeh Arashti^b, Saeed Hesami Tackallou^c, Babak Zamani^d

^aDepartment of Physics, Maybod Branch, Islamic Azad University, Maybod, Iran

^bDepartment of Physics, Yadegar-e-Imam Khomeini (RAH) Shahre Rey Branch, Islamic Azad University, Tehran, Iran

^cDepartment of Biology, Central Tehran Branch, Islamic Azad University, Tehran, Iran

^dDepartment of Physics, Central Tehran Branch, Islamic Azad University, Tehran, Iran

ARTICLE INFO

Article history:

Received: 26 November 2023

Revised: 28 December 2023

Accepted: 30 December 2023

Keywords:

Al film

Fractal

Substrate

AFM

ABSTRACT

In this paper, Al films were deposited on glass and steel substrates by using thermal evaporation technique. X-ray diffraction (XRD) analysis was used for structural characterization of Al thin films. It was found that the growth process mechanism of Al film on two substrates was different. The difference in the growth mechanism and microstructures affects the surface properties. Atomic force microscope (AFM) and field emission scanning electron microscope (FESEM) have been used to describe the surface morphology and fractal properties of Al films. The fractal properties obtained by autocorrelation function (ACF), height-height correlation function (H(r)) and Minkowski function are described and compared with each other. The results of 2D AFM images show that the Al film on the steel substrate has higher surface roughness, roughness exponent, and lateral correlation length compared to the glass substrate. However, the Al film on the glass substrate has a higher spatial complexity with a fractal dimension of $D_f = 2.88$.

1. Introduction

Aluminum (Al) has attracted the attention of many researchers due to its low resistivity, low price, stability, and good adhesion to materials such as glass, steel, silicon, etc. [1, 2]. Al thin films and their alloys are widely used for many applications such as optical sensors, solar cells, thin photovoltaic films, etc. [3-5]. There are several suitable methods for growing Al thin film, such as sublimation, sputtering, pulsed laser deposition, and thermal evaporation [6-8]. Thermal evaporation is a widely used method for the deposition of thin metal layers.

Today, thin film engineering is used in modern technologies. Therefore, it is important to study the surface properties of films using various imaging techniques such as scanning tunneling microscopy (STM), atomic force microscopy (AFM), and transmission electron microscopy (TEM) [9-13]. AFM is a widely used technique to investigate the surface properties of thin films [14]. The surfaces of thin

films have irregularities and the surface roughness is different in various magnifications. Therefore, the rough surface exhibits fractal properties that can be characterized by fractal parameters.

Nasehnejad et al. [15] have shown that the multiscale property of surface roughness and the complexities of surface mechanism can be described by fractal geometry. Therefore, one can have a more accurate and better understanding of the morphological effects on the physical properties of the surface. The fractal dimension (D_f) is a scale-independent parameter that can be used to describe surface complexities. Khachatryan et al [16] investigated the effect of different substrates on Al thin films. They confirmed that the type of substrate and deposition conditions affect the growth of Al films and can produce a crystalline or amorphous structure. Therefore, their physical properties change depending on the type of substrate. In previous works [17, 20], our research group

* Corresponding author.

E-mail address: Mahsa.Fakharpour@iau.ac.ir

Cite this article as:

Fakharpoura, M.*, Gholizadeh Arashti, M., Hesami Tackallou, S. and Zamani, B., 2023. Surface characterization of Al thin film dependent on the substrate using fractal geometry. *Progress in Physics of Applied Materials*, 3(2), pp. 177-183. DOI: [10.22075/PPAM.2023.32439.1069](https://doi.org/10.22075/PPAM.2023.32439.1069)

© 2023 The Author(s). Journal of Progress in Physics of Applied Materials published by Semnan University Press. This is an open access article under the CC-BY 4.0 license. (<https://creativecommons.org/licenses/by/4.0/>)

investigated the effect of substrate type on various properties such as electrical, optical, and mechanical properties of Al thin films.

In this research, the fractal properties and the microstructure of Al film surface on glass and steel substrates are studied. The main aim of this study was to estimate the effect of substrate type on the morphology and topography of Al film. In particular, the effect of surface roughness and layer growth mechanism was investigated for Al films deposited on glass and steel substrates.

2. Experimental

Al thin films on glass and stainless steel substrates were deposited by a vacuum thermal evaporation system in a Hind-HIVAC coating unit (Model of ISF6) with pressure of 1.5×10^{-6} torr (Figure 1). Al pellets of the Merck brand with a purity of 99.99% were placed as an evaporation source in a tungsten evaporation boat. The glass substrate 10 mm×10 mm and steel plate 18 mm×18 mm size were selected. Before deposition, the substrates were ultrasonically cleaned in acetone and ethanol bath for 30 min. During the deposition process, the deposition rate was set at 1 Å/s. The thickness of the Al thin film was controlled by the quartz crystal controller connected to the deposition system to achieve a thickness of 500 nm. The surface topography measurements of the samples were measured on a 5µm scale using an Atomic Force Microscope (AFM) instrument (NanoScope III from Digital Instruments, USA) analysis with a Si tip of 10 nm in diameter on contact mode. AFM images of 256 × 256 pixels were obtained with a scan area of $5 \times 5 \mu\text{m}^2$ at five different locations on each sample. The AFM images were analyzed using the open-source Gwyddion 2.64 software. The crystallite structures of the Al films on glass and steel substrates were measured by X-ray diffraction (XRD) technique with a D8-Advance Bruker instrument equipped with a Cu- α radiation source with $\lambda = 1.5406 \text{ \AA}$ in the scan range of 2θ between 35° and 85° with a step size 0.05. The surface texture of Al films in this study was probed using a field emission scanning electron microscope (FESEM) (Hitachi S-4100 SEM).

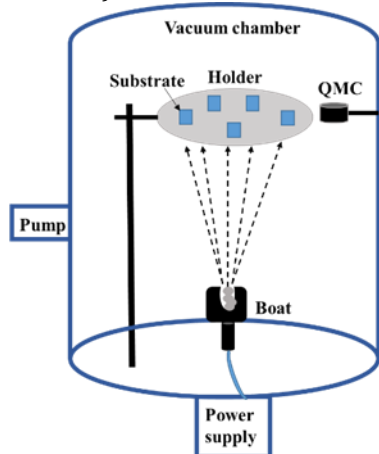


Fig. 1. Schematic of vacuum thermal evaporation system.

3. Results and discussion

Fig. 2(a-b) shows the XRD analysis of Al thin film on glass and steel substrates. As seen in Figure 2a, the peaks at $2\theta=38.4^\circ$, 44.7° , 65.1° , and 78.2° for Al thin film on glass substrate are compatible with card number of JPCD 01-085-1327. The preferred direction of growth is indicated by the strong peak at $2\theta=38.4^\circ$ and in the (111) diffraction plane. The fluctuations created in the X-ray diffraction spectrum can be due to the low thickness of the film and the effect of the glass substrate. Figure 2b shows the diffraction peaks of the Al thin layer on the steel substrate. The Al film on the steel substrate shows two diffraction peaks at angles of $2\theta=38.6^\circ$ and 44.7° , corresponding to card number JPCD 01-085-1327. The peak at $2\theta=50.9^\circ$ is attributed to the steel substrate, which appeared in the diffraction spectrum due to the low thickness of the film. The strongest peak at $2\theta=74.8^\circ$ is attributed to Al_2O_3 which presents preferential growth orientation at the plane of (208). The different peaks in the XRD spectrum for both Al films show that the growth direction of film on the glass substrate occurred in the (111) diffraction plane, while on the steel substrate it occurred in the (208) plane. Since the deposition is performed in vacuum, the appearance of the Al_2O_3 peak may be due to oxidation of the film surface. In addition, the degree of crystallinity of the Al thin film on the steel substrate is higher than that of the glass substrate, which indicates the effect of the substrate on the thin film. In the deposition of thin film, it is necessary for grains to grow on the substrate, and how the grains grow depends on the initial nucleation. If the substrate has a good crystallinity, the thin film will also have a high degree of crystallinity, and if the substrate has an amorphous structure, the film will not have a good degree of crystallinity. The crystallite size of Al film on glass and steel obtained 59.2 nm and 47.6 nm, respectively using Scherrer's equation.

Fig. 3(a-b) shows FESEM images of the surface morphology of Al thin film on glass and steel substrates. The morphology and distribution of grains on both substrates are different. The grains on the glass substrate are polygonal while the grains on the steel substrate are oval. In addition, the distribution of grains on the glass substrate is more uniform than that of steel, which may be due to the conductivity of steel causing the grains to heat up and move along the deposition. Also, the grains on the glass substrate have a larger size than steel. Khachatryan et al. [16] showed that the growth of grains on steel takes place in two stages. First, islands are formed and then these islands grow to create cross-grained layers. In the next step, the voids must be filled by secondary nucleation to form a continuous film. However, the growth of grains on the glass substrate is single-stage and the islands form a continuous film.

The surface and microstructure properties of Al thin films on glass and steel substrates were analyzed by AFM. 2D and 3D AFM images and grain size distribution histograms for Al thin films on glass and steel substrates are shown in Figure 4. The surface of the Al film on both substrates has a heterogeneous morphology with peaks and valleys of several nanometers in height describing the rough surfaces. The grain size (D) was obtained from 2D AFM images using J-microvision software (Figure 4(a-b)).

The grain size of Al thin film on a glass substrate was measured to be larger than that on steel one which is consistent with the FESEM images. The grain sizes obtained from AFM images for Al films on glass and steel are 167.70 nm and 128.04 nm, respectively. Grains on glass have larger sizes compared to steel, which is consistent with the XRD results. Note that crystallite size and grain size can be measured from the XRD spectrum and AFM images, respectively.

3D AFM images (Figure 4(c-d)) show that both thin films have a continuous surface structure. However, the surface of the Al thin film synthesized on the glass substrate has peaks with higher heights compared to the steel substrate. Figure 4(e-f) shows the height distribution density $\rho(z)$ in terms of peak height (Z) of AFM micrographs. The results of height distribution density show that the Al thin film on the steel substrate has a Gaussian distribution with a sharper peak compared to that on the glass. However, the Al thin film on the glass substrate has peaks with various heights compared to steel.

The root mean square roughness (S_q) and average roughness (S_a) indicate the global roughness of the surface. The statistical results calculated for Al thin films on both glass and steel substrates are used from reference [21]

which are given in Table 1. The S_a values are 37.02 nm and 48.49 nm for Al film on glass and steel, respectively. The S_q values are 41.47 and 54.37 nm for Al film on glass and steel, respectively. The results show that the grain size (D_{AFM}) and roughness of the Al film on the steel substrate is greater than that of glass, which may be due to how the grains grow on different substrates. Statistical parameters were used to study the distribution of peaks and valleys (roughness) and their continuity. The skewness (Ssk) value for Al thin film on both substrates is positive, which indicates the predominance of peaks over valleys on the surface [22]. The kurtosis (Kur) value is negative for Al thin film on glass substrate, while it is positive for steel substrate. Therefore, the height distribution on the glass substrate has a higher degree of peakedness, while it has a higher degree of flatness on the steel substrate than the normal distribution. The one-dimensional scans of surface profiles obtained from two arbitrary lines of 2D AFM images for Al films on both glass and steel substrates are shown in Figure 5. The y-axis is in height and the x-axis is in lateral distance ξ . The surface profile includes peaks and valleys that express the different roughness and lateral distance of the two surfaces, which are unevenly distributed on both surfaces.

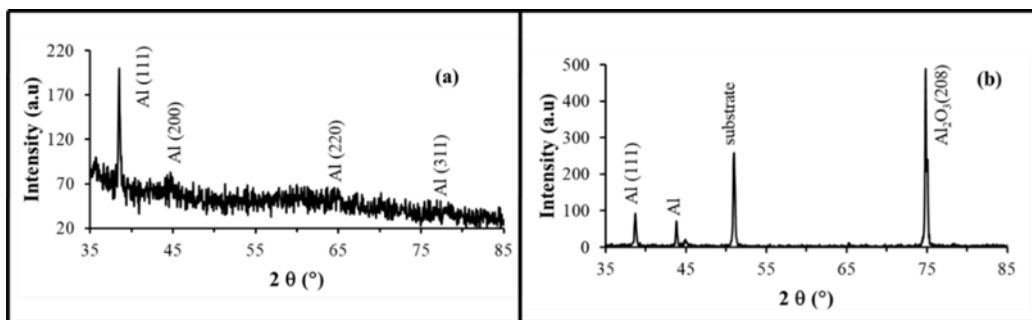


Fig. 2. XRD diffraction patterns for Al thin films on a) glass and b) steel substrates.

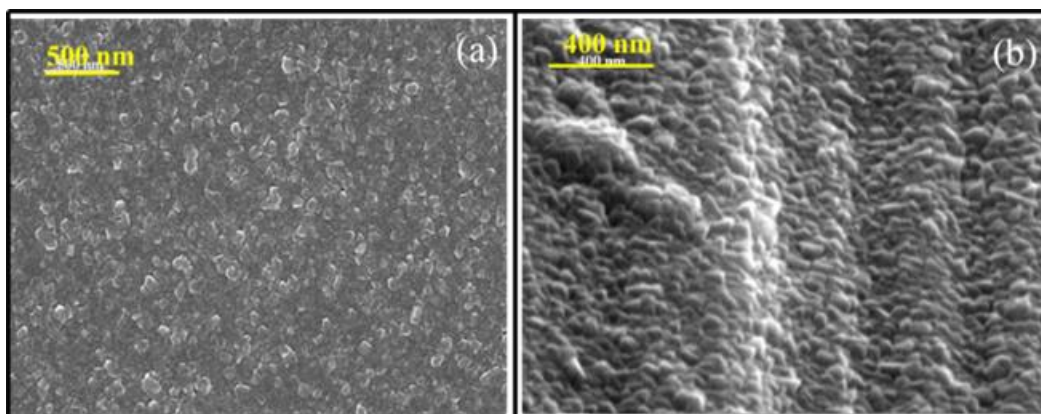


Fig. 3. FESEM images of Al thin films surface on (a) glass, (b) steel substrates.

Table 1. Statistical analyses of Al zigzag thin on glass and steel substrates.

Substrate	D _{AFM} (nm)	S _q (nm)	S _a (nm)	S _{sk}	Kur
Glass	167.70	41.47	37.02	0.077	-0.45
Steel	128.04	54.37	48.49	2.02	7.21

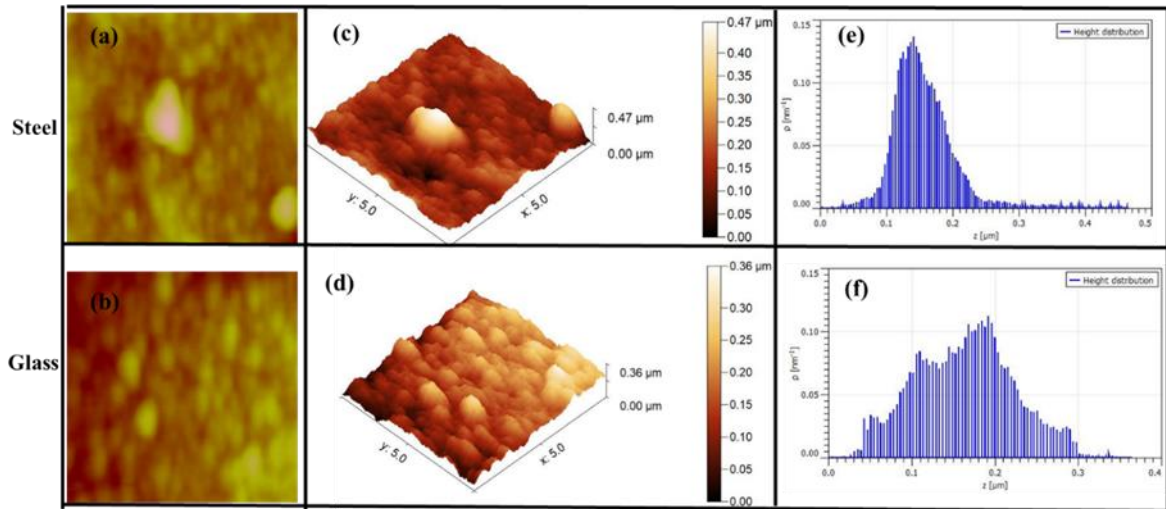


Fig. 4. AFM images of Al thin film on the different substrates; (a-b) 2D images (c-d) 3D images (e-f) height distribution

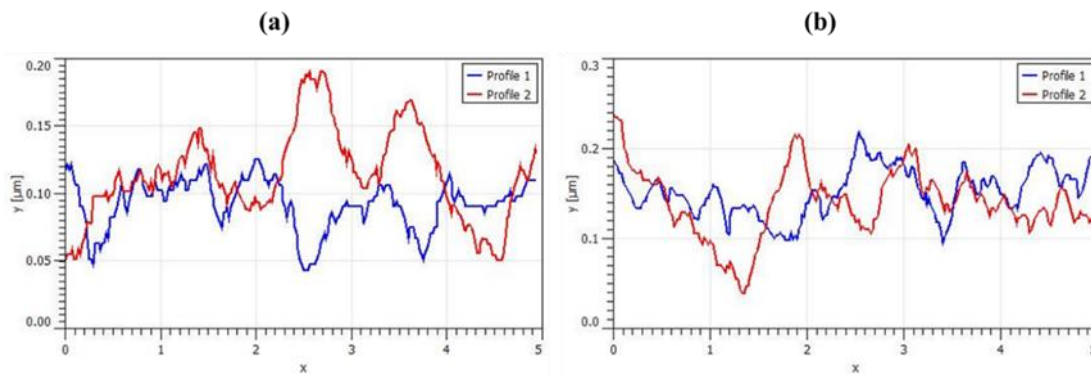


Fig. 5. One-dimensional AFM surface profile scans for Al thin films on a) glass, and b) steel.

To further study the surface and fractal properties of Al thin films on glass and steel layers, from the statistical functions of height-height correlation function ($H(r)$) and correlation function (ACF), and to check the topography and morphology of peaks and valleys from measurements 2D Minkowski is used [23]. The function $H(r)$ is used to describe the rough surfaces of the thin film. The $H(r)$ is defined as [23]:

$$H(r) = 2W^2 \left\{ 1 - \exp \left[- \left(\frac{r}{\xi} \right)^{2\alpha} \right] \right\} \tag{1}$$

where α is known as the roughness exponent and represents the fractality of the surface. The $\log H(r)$ versus

$\log r$ for Al thin films on both substrates is shown in Figure 6. The value of α is obtained from the slope of the linear portion of the graph known as the roughness exponent. Noise in the fixed part of the graph indicate large valleys and peaks on the surface [24]. The separation of two parts in the $\log H$ as a function of the $\log r$ curve describes the self-affine nature of the surface [25]. For the fix part of the curve $H=2w^2$ and the surface global roughness or interface width (w or S_q) can be obtained. The lateral correlation length ξ can be obtained from the intersection of the linear and stable parts of the $\log H$ as a function of the $\log r$ curve. The α indicates the local roughness or smoothness of the surface, with larger values of α describing local smoothness and smaller values describing local roughness [26]. The roughness exponent α is directly related to the fractal

dimension (D_f) as $D_f=3-\alpha$. The variation of the normalized profile length according to the observation scale is described by D_f . Yadav et al [27] reported the relationship between roughness and fractal dimension. The behavior of Al thin films on both glass and steel substrates is similar and it can also be seen that $\log H$ is lower for Al thin film on glass than on steel. The estimated results are listed in Table 2. The α calculated from the plot of $\log H$ versus $\log r$ for Al films on both substrates of glass and steel are 0.12 and 0.26, respectively. Thus, the Al film on steel has a higher roughness exponent in small r regions. Therefore, the fractal dimension depends on the type of depositional substrate. In addition, the Al film on the steel substrate has higher ξ values compared to the steel. This means that similar properties are being repeated. The values of surface roughness W obtained from $\log H$ versus $\log r$ graph for both substrates are different. The W for Al films on glass and steel substrates are 43.86 nm and 55.78 nm, respectively, which are consistent with the results of FESEM and AFM images [16].

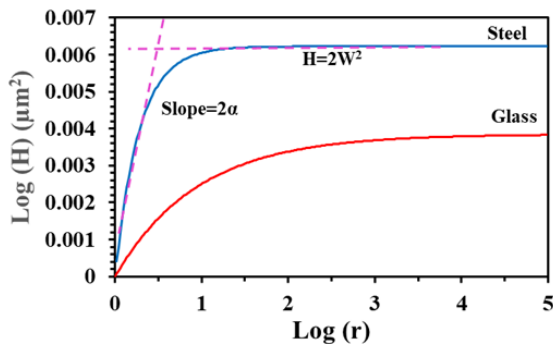


Fig. 6. $\log(H)$ versus $\log(r)$ Al thin films on glass and steel substrates.

The autocorrelation function is used to correlate the surface heights, which is defined as follows [27]:

$$ACF(r = md) = w^{-2} \langle h(i + m, j) \cdot h(i, j) \rangle \quad (2)$$

where d and m are the horizontal distance between two adjacent points and the number of points, respectively. The lateral correlation length ξ is calculated from $1/e$ of the ACF function, which fluctuates for large values of this parameter. The ACF for the surfaces of Al films on glass and steel substrates is shown in Figure 7. The ξ obtained for Al films on glass and steel is 0.28 and 0.31, respectively, which is consistent with the results of the $H(r)$ function. Also, the surface of Al film on steel has a higher roughness compared to glass substrate. The results obtained are given in Table 2. The Al films can form self-affinity surfaces on various substrates with surface complexities as reported by Abhijeet et al. [28].

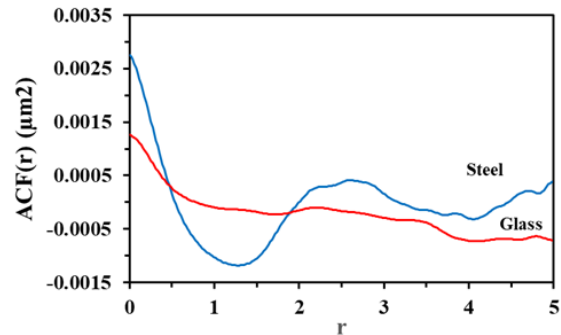


Fig. 7. Autocorrelation function ACF versus r for Al films on glass and steel substrates.

Table 2. Fractal properties of Al films on steel and glass using the height-height correlation function ($H(r)$) and autocorrelation function (ACF).

Substrate	ACF		H(r)		α	$D_f=3-\alpha$
	w [nm]	ξ [nm]	w [nm]	ξ [nm]		
Glass	39.32	0.28	43.86	0.25	0.12	2.88
Steel	52.19	0.31	55.78	0.27	0.26	2.74

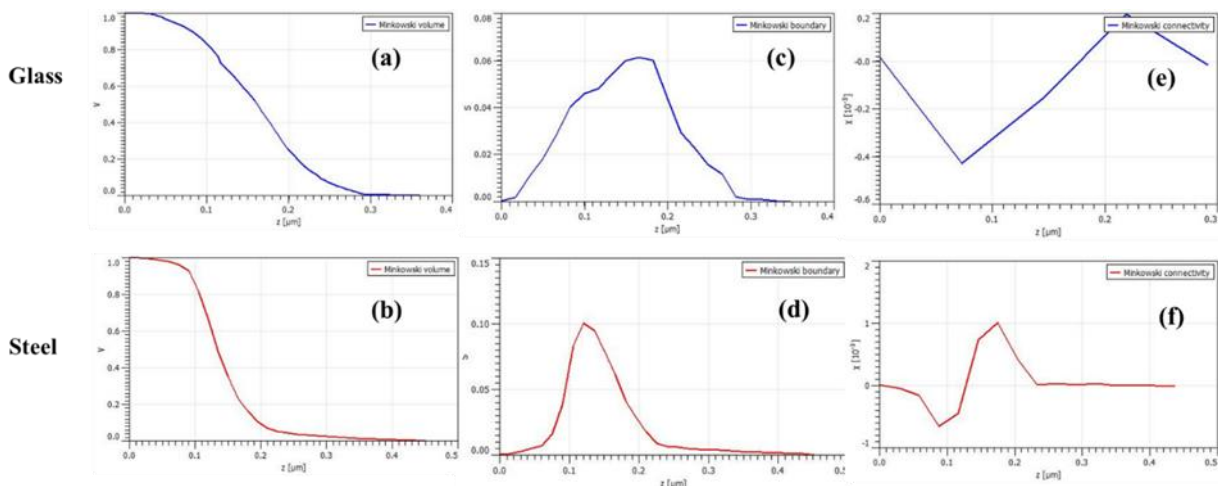


Fig. 8. The Minkowski functionals of a-b) volume $V(z)$, c-d) boundary length $S(z)$, and e-f) connectivity $\chi(z)$ of Al films on glass and steel substrates for the scanning areas of $5 \mu\text{m} \times 5 \mu\text{m}$.

To further study, the local and general surface morphology of films, Minkowski functionals (MFs) have been used. The amount of surface occupation by the substance is described by the volume $V(z)$, the distribution of the surface heights by the boundary length $S(z)$ and the connections of the heights with the Euler-Poincaré characteristic $\chi(z)$ are described by the MFs.

The Gwyddion 2.64 software can be used for the calculation and plotting of the input parameters [29]. Figure 8 shows 2-D Minkowski functionals, volume (V), boundary length (S), and connectivity or Euler characteristic (χ) for Al film on glass and steel substrates. As explained above, the Minkowski functional V describes how the surface is covered. As seen in Figure 8(a-b), the Minkowski volume is symmetric for Al films on both substrates of glass and steel. The symmetry of the Minkowski volume for Al film on both substrates suggests that they have similar topological properties despite having different surface coverages. The Minkowski boundary length (S) measures the length of the boundary between the foreground and background regions in a binary image. S is a measure of the total length of the surface between the two regions and provides information about the surface morphology of the film. A film with a high value of S would have a more complex and irregular surface morphology, while a film with a low value of S would have a smoother and simpler surface morphology. In Figure 8(c-d), the boundary length of Al film on steel substrate is higher than that on glass substrate. Therefore, its surface properties are more complex. The χ is a measure of the topological pattern or fractal nature of the micrograph. The χ can be positive, negative, or zero. The positive and negative χ values indicate dominant peaks and valleys, respectively, while a zero value indicates their uniform distribution. As can be seen in Figure 8(e-f), the plot of the Minkowski connectivity $\chi(z)$ has an oscillatory shape for the surface of Al films on both substrates. The positive and negative values of χ are observed for Al films on both substrates. The results of this work show that the surface morphology of the films can be controlled by changing the substrate.

4. Conclusion

Al thin films were deposited on two substrates of glass (amorphous and non-metallic) and steel (crystalline and metallic). XRD results showed that the Al thin film on steel had a higher degree of crystallinity. FESEM images of the surface of the Al films showed that the grain growth on the glass substrate was continuous, while it was continuous and cross-grained on the steel substrate. Statistical and fractal analyses of the surfaces were performed using 2D AFM images and it was observed that the Al film on the steel substrate had more roughness compared to the steel substrate. The data proved that the substrate could affect the surface morphology of the Al thin film.

Acknowledgements

There is nothing to acknowledge.

Conflicts of Interest

The author declares that there is no conflict of interest regarding the publication of this article.

References

- [1] Mwema, F.M., Oladijo, O.P., Akinlabi, S.A. and Akinlabi, E.T., 2018. Properties of physically deposited thin aluminium film coatings: A review. *Journal of alloys and compounds*, 747, pp.306-323.
- [2] Khlayboonme, S.T. and Thowladda, W., 2021. Impact of Al-doping on structural, electrical, and optical properties of sol-gel dip coated ZnO: Al thin films. *Materials Research Express*, 8(7), p.076402.
- [3] Lambert, A.S., Valiulis, S.N., Malinick, A.S., Tanabe, I. and Cheng, Q., 2020. Plasmonic biosensing with aluminum thin films under the Kretschmann configuration. *Analytical chemistry*, 92(13), pp.8654-8659.
- [4] Moumen, A., Kumarage, G.C. and Comini, E., 2022. P-type metal oxide semiconductor thin films: synthesis and chemical sensor applications. *Sensors*, 22(4), p.1359.
- [5] Manthrammel, M.A., Shkir, M., Anis, M., Shaikh, S.S., Ali, H.E. and AlFaify, S., 2020. Facile spray pyrolysis fabrication of Al: CdS thin films and their key linear and third order nonlinear optical analysis for optoelectronic applications. *Optical Materials*, 100, p.109696.
- [6] Wójcicka, A., Fogarassy, Z., Rácz, A., Kravchuk, T., Sobczak, G. and Borysiewicz, M.A., 2022. Multifactorial investigations of the deposition process–Material property relationships of ZnO: Al thin films deposited by magnetron sputtering in pulsed DC, DC and RF modes using different targets for low resistance highly transparent films on unheated substrates. *Vacuum*, 203, p.111299.
- [7] Kim, K.B., Lee, J. and Kim, M., 2021. Characteristics by deposition and heat treatment of Cr and Al thin film on stainless steel. *Journal of Convergence for Information Technology*, 11(3), pp.167-173.
- [8] Hwidi, M.H., Abduljabbar, L.M. and Emad, A., 2019. Laser effect on optical and structural properties of CdTe: Al thin films prepared by pulsed laser deposition technique. *J Eng Appl Sci*, 14(7), pp.2302-2308.
- [9] Raoufi, D. and Faegh, H., 2012. Surface morphology dynamics in ITO thin films. *Journal of Modern Physics*, 2012.
- [10] Rodríguez-Cañas, E., Aznárez, J.A., Oliva, A.I. and Sacedón, J.L., 2006. Relationship between the surface morphology and the height distribution curve in thermal evaporated Au thin films. *Surface science*, 600(16), pp.3110-3120.
- [11] Fakharpour, M., 2021. The effect of slope and number of arms on the structural properties of square tower-like manganese thin films. *Journal of Nanoanalysis*, 8(1), pp.7-16.
- [12] Karimzadeh, I., Aghazadeh, M., Dalvand, A., Doroudi, T., Kolivand, P.H., Ganjali, M.R. and Norouzi, P., 2019. Effective electrosynthesis and in situ surface coating of Fe₃O₄ nanoparticles with polyvinyl alcohol for biomedical applications. *Materials Research Innovations*, 23(1), pp.1-8.
- [13] Aghazadeh, M., Karimzadeh, I. and Ganjali, M.R., 2019. PVA and EDTA grafted superparamagnetic Ni doped iron oxide nanoparticles prepared by constant current

- electrodeposition for biomedical applications. *Journal of Nanoanalysis*, 6(2), pp.138-144.
- [14] Pinto, E.P., Matos, R.S., Pires, M.A., Lima, L.D.S., Țălu, Ș., da Fonseca Filho, H.D., Ramazanov, S., Solaymani, S. and Larosa, C., 2023. Nanoscale 3D spatial analysis of zirconia disc surfaces subjected to different laser treatments. *Fractal and Fractional*, 7(2), p.160.
- [15] Nasehnejad, M., Nabiyouni, G. and Shahraki, M.G., 2017. Morphological characterisation and microstructure of silver films prepared by electrodeposition method. *Surface Engineering*, 33(5), pp.389-394.
- [16] Khachatryan, H., Lee, S.N., Kim, K.B., Kim, H.K. and Kim, M., 2018. Al thin film: The effect of substrate type on Al film formation and morphology. *Journal of Physics and Chemistry of Solids*, 122, pp.109-117.
- [17] Fakharpour, M. and Taheri, G., 2020. Fabrication of Al zigzag thin films and evaluation of mechanical and hydrophobic properties. *Applied Physics A*, 126(8), p.631.
- [18] Arashti, M.G. and Fakharpour, M., 2020. Fabrication and characterization of Al/glass zig-zag thin film, comparing to the discrete dipole approximation results. *The European Physical Journal B*, 93, pp.1-6.
- [19] Fakharpour, M., Gholizadeh Arashti, M. and Musazade Meybodi, M.T., 2021. Electrical characterization of zig-zag Aluminum thin films using experimental and theoretical methods. *Journal of Optoelectronic Nanostructures*, 6(3), pp.25-42.
- [20] Fakharpour, M., 2023. Fractal and structural analysis of the different sculptured Mn-based nanostructures. *Physics Letters A*, 487, p.129136.
- [21] Nogami, K., Kishimoto, K., Hashimoto, Y., Watanabe, H., Hishii, Y., Ma, Q., Niki, T., Kotani, T., Kiwa, T., Shoji, S. and Ohkubo, T., 2022. Self-growth of silver tree-like fractal structures with different geometries. *Applied Physics A*, 128(10), p.860.
- [22] Rawat, S.S., Harsha, A.P. and Khatri, O.P., 2021. Synergistic effect of binary systems of nanostructured MoS₂/SiO₂ and GO/SiO₂ as additives to coconut oil-derived grease: Enhancement of physicochemical and lubrication properties. *Lubrication Science*, 33(5), pp.290-307.
- [23] Raoufi, D., 2010. Fractal analyses of ITO thin films: A study based on power spectral density. *Physica B: Condensed Matter*, 405(1), pp.451-455.
- [24] Yadav, R.P., Kumar, M., Mittal, A.K., Dwivedi, S. and Pandey, A.C., 2014. On the scaling law analysis of nanodimensional LiF thin film surfaces. *Materials Letters*, 126, pp.123-125.
- [25] Li, J.M., Lu, L., Su, Y. and Lai, M.O., 2000. Self-affine nature of thin film surface. *Applied surface science*, 161(1-2), pp.187-193.
- [26] Richardson, C.E., Park, Y.B. and Atwater, H.A., 2006. Surface evolution during crystalline silicon film growth by low-temperature hot-wire chemical vapor deposition on silicon substrates. *Physical Review B*, 73(24), p.245328.
- [27] Yadav, R.P., Kumar, T., Mittal, A.K., Dwivedi, S. and Kanjilal, D., 2015. Fractal characterization of the silicon surfaces produced by ion beam irradiation of varying fluences. *Applied Surface Science*, 347, pp.706-712.
- [28] Das, A., Chawla, V., Matos, R.S., da Fonseca Filho, H.D., Yadav, R.P., Țălu, Ș. and Kumar, S., 2021. Surface microtexture and wettability analysis of quasi two-dimensional (Ti, Al) N thin films using fractal geometry. *Surface and Coatings Technology*, 421, p.127420.
- [29] Nečas, D. and Klapetek, P., 2012. Gwyddion: an open-source software for SPM data analysis. *Open Physics*, 10(1), pp.181-188.